JOURNAL OF OPTOELECTRONICS AND ADVANCED MATERIALS Vol. 10, No. 7, July 2008, p. 1732 – 1739

Particle correlations in anisotropic traps

P. KOŚCIK, A. OKOPIŃSKA[*]
Institute of Physics, Świętokrzyska Academy ul. Świętokrzyska 15, 25-406 Kielce, Poland

We study the two-dimensional system of charged particles in an anisotropic harmonic potential which serves well as a model of a quantum dot. A numerical analysis of the dependence of the one-particle density and the correlation functions on the harmonic frequencies aspect ratio is presented. For the two-particle system we show that in the case of aspect ratio ωy : $\omega x = 2$, when the problem becomes completely separable, the quasi-exact solutions may be obtained at particular values of confinement frequencies. We use the analytically known eigenfunctions to derive the exact results for various correlation characteristics of the system. The frequencies at which the exact solutions exist correspond to the interesting case of weak confinement, where the correlation effects are important and manifest by formation of Wigner molecules.

(Received April 1, 2008; accepted June 30, 2008)

Keywords: Quantum dots, Wigner molecules, Quasi-solvable problems

1. Introduction

Studies of quantum systems trapped in confining potentials attract considerable attention in view of their possible application to quantum computing. Particularly promising are the physically realized systems of charged particles such as quantum dots (QDs) or few-ion systems in electromagnetic traps. In both cases the inter-particle interaction is Coulombic and the confinement may be modeled by a harmonic potential, the anisotropy of which strongly influences the properties of the system. Such a potential not only provides a good approximation of realistic structures but also is convenient from the theoretical point of view since the center-of-mass motion may be separated out. Here we concentrate on the two-dimensional (2D) structures, realized by nanoscale semiconductor QDs containing a tunable number of electrons that are formed by etching techniques or patterning of the gate electrodes [1]. As a simple example of a quantum mechanical system, the QDs are a useful tool for testing approximation techniques in many-body theory. The case of weak confinement (low density limit) where the correlations between electrons become stronger [2] is especially interesting. When the Coulomb interaction dominates, the electrons tend to localize around the classical equilibrium positions, creating ordered spatial structures called Wigner molecules, which are the finite size counterpart to the crystal phase of the electron gas predicted by Wigner [3]. At present the problem of crystallization in circular quantum dots containing many electrons is well understood [4]. The charge distribution in elliptical, square and triangular QDs has been also studied by using the exact diagonalization approach [5]. Especially the properties of QDs containing two electrons have been extensively investigated in the case of circular [6-8], elliptical [9] and polygonal [10, 11] confinement.

In the present work we study the properties of the two-electron QD confined by an anisotropic harmonic potential $V(x,y)=\frac{\omega_x^2}{2}x^2+\frac{\omega_y^2}{2}y^2$ further. The system is separable in two cases: that of $\omega_x= \omega=\omega_\rho$, and that of $\omega_y : \omega_x=2$ (equivalent to the case of $\omega_y : \omega_x = 1/2$, under the exchange of ω_x and ω_y). In the isotropic confinement case of $\omega_x = \omega_y$, the problem of the relative motion separates in polar coordinates. This case was much studied in the literature [12-14] and its quasi-solvability at particular values of frequency ω_ρ has been pointed out [15]. The closed-form solutions may be useful for determining the exact characteristics of the system. In the anisotropic confinement with the aspect ratio $\omega_y : \omega_x = 2$, the problem is separable in parabolic coordinates [9]. Recently we have shown that also in this case the closed-form solutions may be obtained for particular values of frequency ω_x [16]. In this work we use the exact wave functions to determine various characteristics of QDs in both the $\omega_y : \omega_x = 1$ and $\omega_y : \omega_x = 2$ case. Later, we provide an approximate analytical approach that is particularly suitable to study the Wigner crystallization of electrons in a QD with an arbitrary anisotropy. The outline of our work is as follows. In section II we present the theoretical model of a two-electron QD.

In section III we discuss the separable cases and quasi-exact solutions which are used to study various ground state characteristics. The comparison of the harmonic approximation with the exact results is also made. The paper ends with concluding remarks in section IV.

2. Two-electron quantum dot

The Hamiltonian of the QD consisting of two electrons can be written as

$$H=\sum_{i=1}^{2}\left[\frac{p_i^2}{2m_*}+\frac{m_*}{2}(\omega_x^2x_i^2+\omega_y^2y_i^2)\right]+\frac{e^2}{\varepsilon_*|r_2-r_1|},\quad(1)$$

where m_* is the effective electron mass and ε_* the effective dielectric constant. The corresponding Schrödinger equation is given by

$$H\Psi(r_1,r_2)=\varepsilon\Psi(r_1,r_2),\quad(2)$$

After transformation $\hat{x}=x/a_*;\ \hat{y}=y/a_*$, where $a_*=\hbar^2\varepsilon_*/m_*e^2$ is the effective Bohr radius, the equation takes a form

$$\left[\sum_{i=1}^{2}\left[-\frac{1}{2}\Delta_{\hat{r}_i}^2+2\hat{\omega}_x^2\hat{x}_i^2+2\hat{\omega}_y^2\hat{y}_i^2\right]+\frac{1}{|\hat{r}_2-\hat{r}_1|}\right]\Psi(\hat{r}_1,\hat{r}_2),\quad(3)$$
$$=\hat{\varepsilon}\Psi(\hat{r}_1,\hat{r}_2)$$

where $\hat{\omega}_{x,y}=m_*a_*^2\omega_{x,y}/2\hbar$ $\hat{\varepsilon}=\varepsilon/R^*$ and the effective Rydberg constant $R^*=m_*e^4/\hbar^2\varepsilon_*^2$. Notice that the dimensionless parameters $\hat{\omega}_{x,y}$ measure the ratio of the confinement and interaction energies, and $\hat{\omega}_{x,y}\to 0$ corresponds to strong correlation regime. In the following, we skip the hats over the spatial coordinates, frequencies and energies. Introducing center of mass (CM) $\mathbf{R}=1/2\ (r_1+r_2)=(X;\ Y)$ and relative coordinates $r=r_2-r_1=(x;\ y)$; the Hamiltonian splits into $H=H^{\mathbf{R}}+H^{\mathbf{r}}$ with the CM part $H^R=-\nabla_R^2/4+4(\omega_x^2X^2+\omega_y^2Y^2)$ and the relative motion Hamiltonian $H^r=-\nabla_r^2+\left[\omega_x^2x^2+\omega_y^2y^2\right]+\frac{1}{r}$ Upon representing the spatial wave function as the product of CM and relative motion functions

$$\Psi(x,y,X,Y)=\Psi^R(X,Y)\Psi^r(x,y),\quad(4)$$

the equation of motion (3) yields the two equations

$$\left[-\frac{1}{4}\frac{\partial^2}{\partial X^2}-\frac{1}{4}\frac{\partial^2}{\partial Y^2}+4(\omega_x^2X^2+\omega_y^2Y^2)\right]\Psi^R\quad(5)$$
$$=\varepsilon^R\Psi^R$$

$$\left[-\frac{\partial^2}{\partial x^2}-\frac{\partial^2}{\partial y^2}+\omega_x^2x^2+\omega_y^2y^2+\frac{1}{\sqrt{x^2+y^2}}\right]\Psi^r\quad(6)$$
$$=\varepsilon^r\Psi^r$$

where $\varepsilon=\varepsilon^R+\varepsilon^r$. The solution of CM !equation (5) is given by

$$\Psi_{n,m}^R(X,Y)=\frac{2\omega_x^{\frac{1}{4}}\omega_y^{\frac{1}{4}}}{2^{\frac{n}{2}+\frac{m}{2}}\sqrt{\pi}\sqrt{n!}\sqrt{m!}}e^{-2(\omega_xX^2+\omega_yY^2)}\quad(7)$$
$$H_n(2\sqrt{\omega_x}X)H_m(2\sqrt{\omega_y}Y)$$

where H_n is the Hermite polynomial of nth order, and the corresponding energy reads

$$\varepsilon_{n,m}^R=2\omega_x(n+\frac{1}{2})+2\omega_y(m+\frac{1}{2}).\quad(8)$$

The problem is thus reduced to solving the 2D relative motion equation (6), which can be performed numerically. The symmetry under electron exchange requires the spatial wave function to be symmetric or antisymmetric depending on the total spin of the system. As the

CM coordinate remains the same upon the interchange of electrons, the symmetry requirement reduces to the symmetry of the relative wave-function under inversion r → -r. Because of the invariance of equation (6) to reflections about the *x*- and *y*-axis, the (*x*; *y*)-parity of the relative motion spatial wave-functions is well-defined.

In this work we study particularly carefully the two special cases, $\omega_y=\omega_x$ and $\omega_y=2\omega_x$, where the problem can be simplified by separating the variables. In both cases the problem appears quasi-solvable, i.e some solutions can be obtained in closed-form. We will use the exact solutions to study the ground state characteristics in both the isotropic and anisotropic confinement potential.

3. Ground state characteristics

There are various means to examine the characteristics of a quantum system. Here we compare them from the point of view of how well they describe the correlations of the two particles in a harmonic trap. The following characteristics will be discussed: one-particle density, pair correlation function and conditional probability distribution. Below we give the definitions of the considered functions specified for the two-particle system.

1. The *one-particle density* is defined by

$$n(r)=2\int dr_1\left|\Psi^R(\frac{r+r_1}{2})\right|^2\left|\Psi^r(r_1-r)\right|^2,\quad(9)$$

2. The *pair correlation function* (PCF) is given by

$$G(r)=\left\langle\Psi(r_1,r_2)\middle|\sum_{i\langle j}^{2}\delta(r_i-r_j-r)\middle|\Psi(r_1,r_2)\right\rangle\quad(10)$$
$$=\left|\Psi^r(r)\right|^2$$

3. The *conditional probability distribution* (CPD) determines the probability for finding one particle at r = (*x; y*) given that the other is at r$_0$ = (x_0; y_0). For the two particle system CPD is just proportional to the modulus squared of the wave-function

$$\left|\Psi(r_0,r)\right|^2$$

$$P(r,r_0)=\frac{\left|\Psi^r(r-r_0)\right|^2\left|\Psi^R(\frac{r+r_0}{2})\right|^2}{\int dr\left|\Psi^r(r-r_0)\right|^2\left|\Psi^R(\frac{r+r_0}{2})\right|^2} \qquad (11)$$

A. Exact results

1. Isotropic confinement potential $\omega_y = \omega_x = \omega_\rho$

In the circularly symmetric case, the Schrödinger equation in polar coordinates ($\rho;\varphi$) is transformed into

$$\left[-\left(\frac{\partial^2}{\partial\rho^2}+\frac{1}{\rho}\frac{\partial}{\partial\rho}\right)+\frac{\hat{L}_z^2}{\rho^2}+\omega_\rho\rho^2+\frac{1}{\rho}\right]\Psi^r(\varphi,\rho) \qquad (12)$$
$$=\varepsilon^r\Psi^r(\varphi,\rho)$$

By substituting $\Psi^r(\varphi,\rho)=e^{im\varphi}u^r(\rho)/\sqrt{\rho}, m=0,\pm1,...$ in the above, we get the radial equation

$$\left[-\frac{d^2}{d\rho^2}+\frac{m^2-\frac{1}{4}}{\rho^2}+\omega_\rho^2\rho^2+\frac{1}{\rho}\right]u^r(\rho) \qquad (13)$$
$$=\varepsilon^r u^r(\rho)$$

The quasi-exact solutions to the above equation found by Taut [15] may be enumerated by integer numbers *n*. In this work we consider the four lowest values of *n*, for which the exact wave functions correspond to ground states. The values of confinement frequencies

$$\omega_\rho^{n=1}=\frac{1}{2}=0.5$$
$$\omega_\rho^{n=2}=\frac{1}{12}\approx 0.0833$$
$$\omega_\rho^{n=3}=\frac{1}{54}(10-\sqrt{73})\approx 0.0270$$
$$\omega_\rho^{n=4}=\frac{1}{656}(25-3\sqrt{33})\approx 0.0118 \qquad (14)$$

are determined by the procedure described in the Appendix, where the corresponding wave functions can be also found. It turns out that $\omega_\rho^{n=1}=\frac{1}{2}$ is the largest value of confinement frequency at which the exact solution is known.

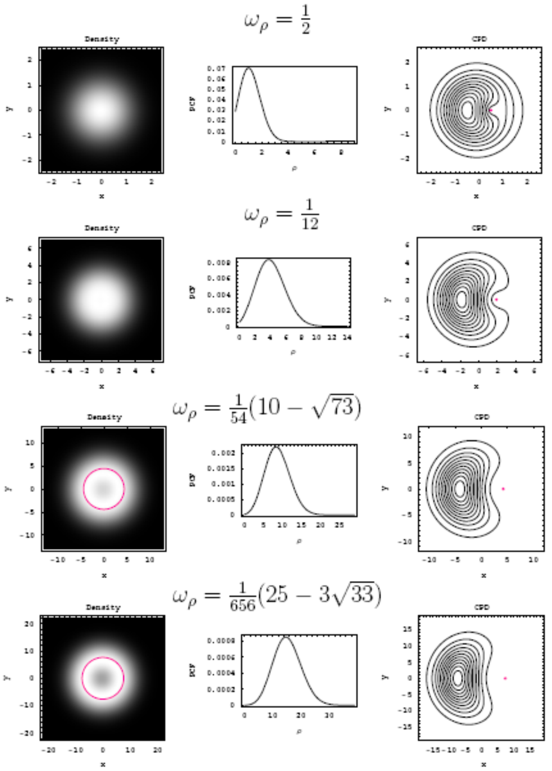

Fig. 1. Charge density, PCF and CPD for the two-electron QD in the case of isotropic confinement

In Fig. 1 we have plotted the density, PCF and CPD in the above four cases. The one-particle density (plotted in the left column) and the PCF (plotted in the midle column) are circularly symmetric. It can be noted that for decreasing ω_ρ, the maximum of the charge density moves from ρ= 0 to the circle of a radius $\rho_{cl}/2$, where $\rho_{cl}=1/2^{\frac{1}{3}}\omega_\rho^{\frac{2}{3}}$ is the classical equilibrium distance between Coulomb interacting particles in the trap. Similarly, we may observe how the radius ρ_{max}, at which the PCF attains a maximum, shifts toward ρ_{cl}=2.

The most informative picture is obtained from the CPD if the reference particle is fixed at its most probable position, namely in the point r$_{mp}$ = (ρ_{max}/2,0), where ρ_{max} is determined from the maximum of the PCF. The CPD in function of the position of the second electron r, namely *P*(r; r$_{mp}$), plotted in the right column of Fig.1, clearly shows that for ω_ρ < 0.01, a Wigner molecule is formed. Observe that the Wigner crystallization does not show up in the density plot, because the charges of separate particle are not distinguishable in the rotationally invariant electron density. This corresponds to the fact that the lowest classical configuration is infinitely degenerate with respect to rotations around the center of the trap.

2. Confinement potential with anisotropy $\omega_y : \omega_x = 2$

In the case of anisotropic confinement the only separable case is that of ω_y=2ω_x. In 2D parabolic coordinates

$$x = \eta_1\eta_2, y = \frac{1}{2}\left(\eta_1^2 - \eta_2^2\right)\eta_2 \geq 0, \quad (15)$$

the Schrödinger equation (6) is transformed into the form

$$\frac{1}{\eta_1^2+\eta_2^2}\Big[-\frac{\partial^2}{\partial\eta_1^2} - \frac{\partial^2}{\partial\eta_2^2} + \frac{1}{4}\omega_y^2(\eta_1^6+\eta_2^6) - \frac{1}{4}\eta_1^2\eta(\eta_1^2+\eta_2^2)(\omega_y^2-4\omega_x^2)+2 \Big]\Psi(\eta_1,\eta_2) \quad (16)$$
$$= \varepsilon^r\Psi(\eta_1,\eta_2)$$

For ω_y=2ω_x the above equation is solved by $\Psi(\eta_1,\eta_2) = g_1(\eta_1)g_2(\eta_2)$ and the relative motion problem is separated into the two ordinary differential equations of the identical form

$$\Big[-\frac{d^2}{d\eta_j^2} - \varepsilon^r\eta_j^2 + \omega_x^2\eta_j^6 + \beta_j \Big]g_j(\eta_j) = 0, j = 1.2, \quad (17)$$

which are coupled by the condition β_1+β_2 = 2 to be satisfied by the separation constants β_1 and β_2 . Bound-state solutions are obtained at the values of ε^r and β_j such that the functions $\Psi(\eta_1,\eta_2)$ vanish, as $|\eta_1|, \eta_{2\to\infty}$.
The ground state solutions, in which we are interested in the present work, correspond to the case of β_1 = β_2 = 1 and the functions $g_j(\eta_j)$ not having the nodal points.
As we have recently shown, the coupled equations (17) appear quasi-solvable [16]. Th=e solution can be found in closed form for particular values of ω_x that are enumerated by an integer number *n* as discussed in the Appendix. The values of ω_x for *n* = 1*;* 2*;* 3*;* 4 are calculated to be given by

$$\omega_x^{n=1} = \frac{1}{8} = 0.125$$
$$\omega_x^{n=2} = \frac{1}{64} \approx 0.156$$
$$\omega_x^{n=3} = \frac{1}{120}(5-2\sqrt{5}) \approx 0.044$$
$$\omega_x^{n=4} = \frac{1}{1472}(10-3\sqrt{6}) \approx 0.0018 \quad (18)$$

They correspond to ground-states and, similarly as in the case of isotropic confinement, they decrease for increasing *n*. The plots of the density in the above four cases are presented in Fig.2, where the positions of the charges in the classical configuration ((x_{cl}/2, 0), (-x_{cl}/2, 0)) are also marked with $x_{cl} = 1/2^{\frac{1}{3}}\omega_x^{\frac{2}{3}}$ being the classical distance between the electrons. The density is anisotropic, reflecting the shape of the confining potential, and for decreasing ω_x it tends to become spatially separated with Gaussian-like peaks around the classical equilibrium points. The number of density maxima is equal to the particle number, which is the consequence of the fact that the lowest classical configuration of the two-particle system is non-degenerate. This is in difference to the case of isotropic confinement, where the Wigner crystallization does not show up in the density plot.

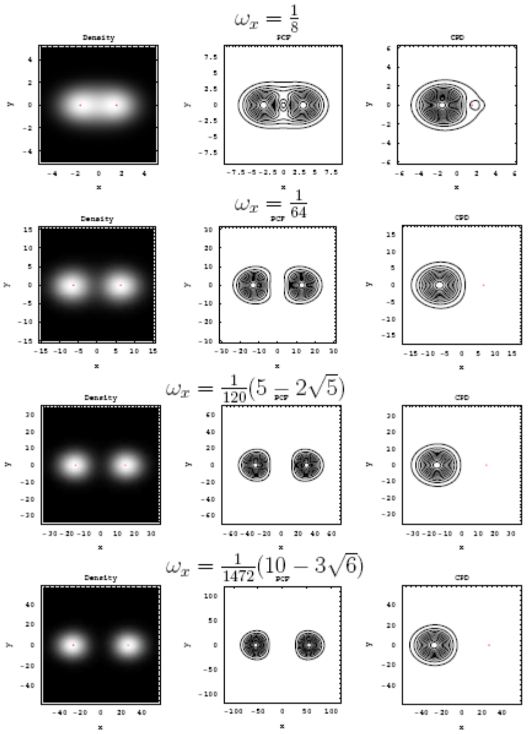

Fig. 2. Charge density, PCF and CPD of the two-electron QD in the case of anisotropic confinement

The PCF is plotted in the middle column of Fig.2, its behavior appears very similar to that of the density, only the distances between the maxima x_{max} are slightly different. In the last column we placed the plots of CPD with the reference electron located in the most probable position r_{mp} = (x_{max}=2*;* 0) as a function of the second electron position *P*(r*;* r_{mp}). In the case of the weakest confinement ($\omega_x^{n=1} = \frac{1}{8}$), the CPD has a maximum in the point (-x_{max}/2, 0) that is diametrical to the position of the reference electron with respect to the center of the trap, but the probability of finding the second electron around the first one is not negligible. This indicates that the molecular-like state is not formed in agreement with the fact that crystallization is not observed in the density plot. For decreasing ω_x, the probability of finding the second electron decreases around the reference electron position creating a correlation hole. The electrons get more and more localized in the vicinity of the points

($x_{max}/2$, 0) and ($-x_{max}/2$,0), which become close to the classical equilibrium point. In the case of $\omega_x^{n=4} \approx 0.0018$ the correlation hole around the reference electron clearly attests the presence of the Wigner crystallization.

3. Correlation measures

The accurate description of an *N*-body interacting system is a difficult task. The Hartree-Fock picture is usually used as a first approximation since it provides a simple way understanding by mapping an interacting system onto a system of non-interacting particles moving in a self-consistent field of other particles. In the one-particle picture, the exchange correlations due to Fermi statistics are accounted for, since the wave function of the system is approximated by a determinant of single electron functions, but the correlations arising from the mutual interaction of electrons are beyond the scope of this approach. The possible ways of including the Coulomb correlations into this picture have been discussed first by Wigner and Seitz [17]. They introduced a quantity called the *correlation energy*, defined by the difference between the exact ground-state energy and its Hartree-Fock approximation

$$E_{corr}=E-E_{HF} \tag{19}$$

which is frequently used until now as an energetic measure of the correlation effect. However, E_{corr} is not a measurable quantity and its determination with the chosen method of ground-state energy calculation is inconvenient as it requires the Hartree-Fock calculation to be additionally performed. In strict sense E_{corr} is not a measure of the true correlation strength but a measure of quality of the HF approximation. This shows up in the fact that E_{corr} does not vanish in the limit of vanishing interaction between electrons [18]. Therefore, various purely quantum-kinematical measures have been considered [19]. The simplest possibility of statistical correlation coeficients has been discussed by Kutzelnigg et al. [20]. Here we consider the *Kutzelnigg coefficient* that is defined as a scalar quantity

$$r = \frac{\langle r_1 \cdot r_2 \rangle - \langle r \rangle^2}{\langle r^2 \rangle - \langle r \rangle^2} \quad , \tag{20}$$

where the expectation values $<r>$ and $<r^2>$ are determined by the one-electron density and $\langle r_1 \cdot r_2 \rangle$ is determined by the two-electron distribution. For the two-electron system the expectation value of a function *f* of one variable r is given by

$$\langle f(r) \rangle = \frac{1}{2} \int f(r) n(r) dr \tag{21}$$

and that of a function *f* of two variables r_1 and r_2 reads

$$\langle f(r_1,r_2) \rangle = \int f(r_1,r_2) |\phi(r_1,r_2)|^2 dr_1 dr_2 \,, \tag{22}$$

Since the origin of coordinate system is chosen in the center of the harmonic trap, Eq.20 simplifies to the form

$$\tau = \frac{\langle r_1 \cdot r_2 \rangle}{\langle r^2 \rangle} = \frac{\langle r_1 r_2 \cos\theta_{12} \rangle}{\langle r^2 \rangle} \,, \tag{23}$$

that shows that $|\,\tau\,| \leq 1$. The Kutzelnigg coeficient vanishes for independent particles, and its limiting values correspond to perfect correlations case, with $\tau = 1$ for coincident electrons positions and $\tau = -1$ for positions diametrical with respect to the center of the trap.

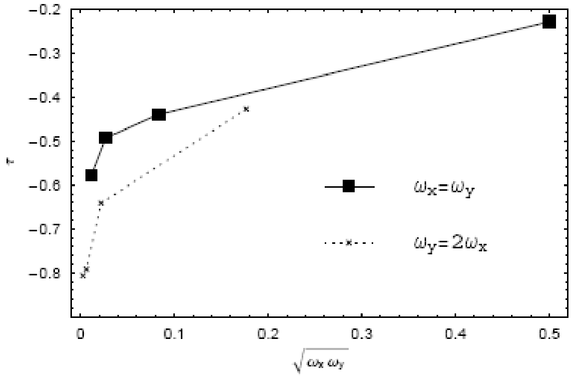

Fig. 3. Kutzelnigg coefficient τ calculated for four exact states in the case of isotropic (full line) and anisotropic confinement (dotted line).

In Fig.3 we plotted the vales of the Kutzelnigg coefficient for the exactly known states of the two-electron QD at the partiycular values of ω_x and ω_y frequencies. In order to compare the isotropic and anisotropic confinement cases, the results are presented in function of the geometric mean of the frequencies, $\sqrt{\omega_x \omega_y}$ that is a measure of confinement strength. For $\sqrt{\omega_x \omega_y} \to 0$, the value of the Kutzelnigg coefficient decreases and tends to the value $\tau = -1$, which corresponds to the perfect Wigner crystallization. We may see that anisotropy increases correlations and the Wigner crystallization occurs at stronger confinement than in the corresponding spherical QDs.

B. Harmonic approximation

We have shown that Wigner crystallization for the circularly symmetric two-electron QD takes place if ω_ρ is smaller than some critical value

$\omega_\rho^{cr} \approx 0.01$. This case has been studied in the harmonic approximation [6] and it has been shown that a qualitatively good description of the strong correlation regime is obtained [6, 8]. We have shown that in the case of anisotropic confinement with the aspect ratio $\omega_x : \omega_y = 1 : 2$, where the exact solutions are available, the critical value ω_ρ^{cr} below which the Wigner crystallization occurs is larger than in the circularly symmetric case. Here we will study the case of anisotropic confinement potential with an arbitrary aspect ratio using the harmonic approximation, which is expected to perform well in the case of weak confinement.

If $\omega_y > \omega_x$, the potential $V(x,y) = \omega_x^2 x^2 + \omega_y^2 y^2 + 1/\sqrt{x^2+y^2}$ in the relative motion equation (6) has two local minima at the classical equilibrium points (x_{cl}, 0) and ($-x_{cl}$, 0). Expansion into a Taylor series around the minimum at $r_{min} = (x_{cl}, 0)$ yields

$$V(x,y) \approx V(r_{\min}) + 3\omega_x^2 (x - x_{cl})^2 + (\omega_y^2 - \omega_x^2) y^2 + \ldots + .. \tag{24}$$

where the first term is a classical dot energy, whilefthe second and third terms give the potential of the shifted oscillator of frequency $\sqrt{3}\omega_x$ and the oscillator of frequency $\sqrt{\omega_y^2 - \omega_x^2}$, respectively. The relative motion equation (6) may be approximated by a soluble Schrödinger equation

$$\left[-\frac{\partial^2}{\partial x^2} - \frac{\partial^2}{\partial y^2} + V(r_{\min}) + 3\omega_x^2 (x - x_{cl})^2 + (\omega_y^2 - \omega_x^2) y^2 \right] \Psi^r = \Psi^r \varepsilon^r \tag{25}$$

the eigenvalues of which are of the form

$$\varepsilon_{n,m}^r = \frac{1}{2}(3(2)^{\frac{1}{3}} \omega_x^{\frac{2}{3}} + 4(\sqrt{3}(\frac{1}{2}+n)\omega_x + (\frac{1}{2}+m)\sqrt{\omega_y^2 - \omega_x^2})) \tag{26}$$

and the eigenfunctions are given by

$$\Psi_{n,m}^r(x,y) = \Psi_n(x)\Psi_m(y) \;, \tag{27}$$

where

$$\Psi_n(x) \sim \mathrm{e}^{-\frac{\sqrt{3}\omega_x}{2}(x-x_{cl})^2} H_n(\sqrt{\sqrt{3}\omega_x}(x - x_{cl})) \tag{28}$$

$$\text{and } \Psi_m(y) \sim \mathrm{e}^{-\frac{1}{2}\sqrt{\omega_y^2-\omega_x^2}\,y^2} H_m(\sqrt{\sqrt{\omega_y^2 - \omega_x^2 y}}\,) \tag{29}$$

The states with well-defined parity ($x; y$) may be constructed as

$$\Psi_{n,m}^r(x,y) = (\Psi_n(x) \pm \Psi_n(-x))\Psi_m(y) \;, \tag{30}$$

where the sign + /- corresponds to the solution that is even/ odd in x.

For gauging the quality of the approximation we solved the relative motion equation (6) numerically with the help of the Rayleigh-Ritz method using the basis of the two-dimensional harmonic oscillator eigenstates. In Fig.4, the bound state energies are plotted for an exemplary value $\omega_x = 1/3$. The structure of the spectrum changes dramatically as ω_y increases since the states with spatial parity (-, +), (+,-) tend to become degenerate with those of (+, +), (-,-), respectively. We may see that the spectrum of (6) is well approximated by the expression (26) in the considered range of ω_y. Observe that each state of the harmonic model provides approximation to the two states, namely the singlet (the same x- and y- parity ((+,+), (-,-)) and the triplet (different x- and y- parities ((-,+), (+,-)), and the approximate energy lies in between the energies of the two states. The approximation becomes exact in the limit of $\omega_y \to \infty$, when the singlet and triplet states become degenerate.

It may be easily checked that for decreasing values of ω_x, the singlet and triplet eigenvalues get close at smaller values of ω_y and the spectrum is better and better approximated by the expression (26).

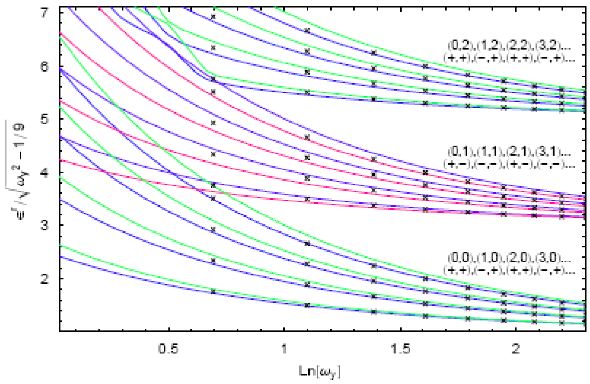

Fig. 4. Bound-state energies of the two-electron QD with confinement frequency $\omega_x = 1/3$ in function of $\mathrm{Ln}\,\omega_y$. The exact energies of the states of parity (+, +),(-, +),(+, +),(-, +) and those of parity (+,-), (-,-),(+,-), (-,-) are compared with the harmonic approximation (n,m) that are marked by crosses. The lines are ordered from below.

Using the wave function (30) for $n,m = 0$, the ground-state density n(x, y) in the harmonic approximation for $\omega_x \ll 1$ may be estimated as

$$n(x,y) \approx Ne^{\frac{-4\omega y\sqrt{\omega_y^2-\omega_x^2 y^2}}{\omega y+\sqrt{\omega_y^2-\omega_x^2}}} e^{-\frac{4\sqrt{3\omega_x}}{1+\sqrt{3}}(x+x_{cl}/2)^2} + e^{-\frac{4\sqrt{3\omega_x}}{1+\sqrt{3}}(x-x_{cl}/2)^2} \quad (31)$$

Then for small ω_x the charge density has the maxima in the points of classical equilibrium ($x_{cl}/2$, 0); ($-x_{cl}/2$, 0). This attests that for ω_x smaller than $\omega_x^{cr} \approx 0.1$ crystallization occurs independently of the value of frequency ω_y.

The harmonic approximation describes also well the local properties of the anisotropically confined system. In Fig.5 we compare the density plot with the exact results for the aspect ratio $\omega_y : \omega_x = 2$ in two cases: that of strong confinement ($\omega_x = 1/8$) and that of weak confinement ($\omega_x = (10 - 3\sqrt{6})=1472$). In both cases the agreement is qualitatively good. For larger anisotropy the performance of the harmonic approximation is even better in accord with the tendency shown in energetic plot of Fig.4.

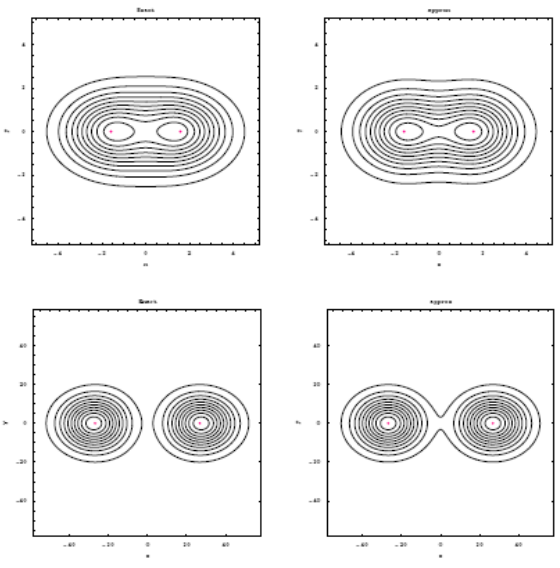

Fig. 5. Comparison of the exact density with the harmonic approximation (31) for the confinement aspect ratio ω_y:ω_x =2 in the cases of ω_x = 1/8 (upper plots) and ω_x = (10 - 3 √6) =1472 (lower plots).

4. Conclusions

We have studied the 2D QD consisting of two interacting electrons confined in an anisotropic harmonic potential. Using the closed-form expressions for wave functions at particular values of confinement strength, the one-particle density and the correlation functions have been obtained in the case of isotropic confinement and in the case of anisotropy aspect ratio $\omega_y : \omega_x = 2$. The frequencies at which the exact solutions exist correspond to the interesting case of weak confinement, which allowed us to study the correlation effects and formation of the Wigner molecules. Various correlation measures have been discussed. By a comparison with the exact results we have shown that the harmonic approximation for the QD with an arbitrary confinement anisotropy performs well in the weak confinement case.

5. Appendix. Quasi-exact solutions

A. Isotropic case: $\omega_y : \omega_x = 1$

The solution of (13) is represented by [15]

$$u^r(\rho) = \rho^{|m|+\frac{1}{2}} e^{-\frac{\omega_\rho}{2}\rho^2} \sum_{i=0}^{\infty} a_i \rho^i \quad (32)$$

where the coefficients a_i satisfy the recurrence relation

$$A_i a_{i+1} + B_i a_i + C_i a_{i-1} = 0 \quad (33)$$

With

$$A_i = (i + 1)(i + 2|m| + 1)$$
$$B_i = -1$$
$$C_i = \varepsilon^r - 2\omega_\rho(i + |m|) \quad (34)$$

The values of ω_ρ, for which the series in (32) terminates after a finite number of terms are determined by solving the pair of algebraic equations

$$Det\begin{pmatrix} B_0 & A_0 & \cdots & \cdots & 0 \\ C_1 & B_1 & A_1 & \cdots & 0 \\ 0 & C_2 & B_2 & A_2 & 0 \\ \cdots & \cdots & \cdots & \cdots & \cdots \\ 0 & \cdots & C_{n-1} & B_{n-1} & A_{n-1} \\ 0 & \cdots & \cdots & C_n & B_n \end{pmatrix} = 0 \quad (35)$$

And

$$\varepsilon^r = 2\omega_\rho(i + n + |m|) \quad (36)$$

at a chosen value of n = 1, 2, …. and a closed-form solution of energy ε^r exists.

$$\Psi^r_{\omega_\rho=\frac{1}{2}}(\rho,\varphi) = \frac{1}{\sqrt{2\pi}} \frac{1}{\sqrt{3+\sqrt{2\pi}}} e^{-\frac{\rho^2}{4}}(1+\rho) \quad (37)$$

$$\Psi^r_{\omega_\rho=\frac{1}{12}}(\rho,\varphi) = \frac{1}{\sqrt{2\pi}} \frac{1}{\sqrt{6(25+8\sqrt{3\pi}}} e^{-\frac{\rho^2}{24}}(1+\rho+\rho^2/6) \quad (38)$$

B. Anisotropic case: $\omega_y : \omega_x = 2$

The solutions of the equations (17) are represented as [16]

$$g(\eta_j \beta_j) = e^{-\frac{\omega_x \eta_j^4}{4}} \sum_{i=0}^{n} a_i^{(j)} \eta_j^{2i+\nu} \quad (39)$$

where $a_0^{(j)} \neq 0$, and ν = 0, 1 correspond to the even-and odd-parity case, respectively. The three-term recursion relation for the expansion coefficients $a_i^{(j)}$ has the form

$$A_i a_{i+1}^{(j)} + B_i^{(j)} a_i^{(j)} + C_i a_{i-1}^{(j)} = 0 \quad (40)$$

Where

$$A_i = (2i + \nu + 1)(2i + \nu + 2)$$
$$B_i^{(j)} = -\beta_j$$
$$C_i = \varepsilon^r + (1 - 4i - 2\nu)\omega_x \quad (41)$$

with $a_i^{(j)} = 0$ for i < 0. The conditions of quasi-solvability for j = 1,2 are of the form

$$Det\begin{pmatrix} B_0^{(j)} & A_0 & \cdots & \cdots & 0 \\ C_1 & B_1^{(j)} & A_1 & \cdots & 0 \\ 0 & C_2 & B_2^{(j)} & A_2 & 0 \\ \cdots & \cdots & \cdots & \cdots & \cdots \\ 0 & \cdots & C_{n-1} & B_{n-1}^{(j)} & A_{n-1} \\ 0 & \cdots & \cdots & C_n & B_n^{(j)} \end{pmatrix} = 0 \quad (42)$$

And

$$\varepsilon^r = \omega_x(3 + 4n + 2\nu) \quad ,(43)$$

with the imposition of $\beta_1+\beta_2 = 2$. These equation determine the values of ω_x for which the closed form solution of Eq. 6 exists. The bound-state energy is given by (43).

The normalized wave function of the relative motion in cartesian coordinates for n = 1 and n = 2, are of the form

$$\Psi^r_{\omega_x = \frac{1}{8}}(x,y) = \frac{1}{2\sqrt{(12\pi\sqrt{2} + \Gamma\left[-\frac{1}{4}\right]^2 + 2\Gamma\left[\frac{1}{4}\right]^2})} \quad (44)$$
$$e^{\frac{-x^2-2y^2}{16}}\left(1 + \frac{1}{4}x^2 + \sqrt{x^2+y^2}\right)$$

$$\Psi^r_{\omega_x = \frac{1}{64}}(x,y) = \frac{1}{32768 * 2^{\frac{3}{4}}\sqrt{25\pi + 3\Gamma\left[\frac{1}{4}\right]^2 + 26\Gamma\left[\frac{3}{4}\right]^2}}$$
$$e^{\frac{-x^2-2y^2}{128}}\left(x^4 + 32x^2(10 + \sqrt{x^2+y^2}) + 128(8 + y^2\right.$$
$$\left. + 8\sqrt{x^2+y^2}\right) \quad (45)$$

References

[1] L. Jacak, P. Hawrylak, A. Wojs, Quantum Dots, Springer, Berlin, 1997.
[2] G.W. Bryant, Phys. Rev. Lett. **59**, 1140 (1987).
[3] E.P. Wigner, Phys. Rev. **46**, 1002 (1934).
[4] P.A. Maksym, H. Immamura, G.P. Mallon, H. Aoki, J.Phys.: Condens. Matter **12**, R299 (2000).
[5] B. Szafran, F. M. Peeters, S. Bednarek, J. Adamowski, Phys.Rev. B **69**, 125344 (2004).
[6] A. Matulis, F.M. Peeters, Solid State Commun. **117**, 655 (2001).
[7] C. Yannouleas, U. Landman, Phys. Rev. Lett. **85**, 1726 (2000).
[8] A. Puente, L.Serra, R.G.Nazmitindov, Phys. Rev. B **69**, 125315 (2004)
[9] P. S. Drouvelis, P. Schmelcher, F. K. Diakonos, Phys. Rev.B **69**, 035333 (2004); Phys. Rev.B **69**, 155312 (2004).
[10] C. E. Creffield, Wolfgang Häusler, J. H. Jefferson, Sarben Sarkar Phys.Rev. B **59**, 10719 (1999).
[11] E. Räsänen, H. Saarikoski, M. J. Puska, R. M. Nieminen, Phys. Rev. B **67**, 035326 (2003).
[12] U. Merkt, J.Huser, M.Wagner, Phys.Rev. B **43**, 7320 (1991).
[13] J.L.Zhu, Phys. Rev. B **55**, 15819 (1997).
[14] R. M. G. García-Castelán, W. S. Choe, Y. C. Lee, Phys.Rev. B **57**, 9792 (1998).
[15] M. Taut, J. Phys. A: Math. Gen. **27**, 1045 (1994).
[16] P. Kościk, A. Okopińska, J. Phys. A: Math. Theor. **40**, 1045 (2007).
[17] E. P.Wigner, F.Seitz, Phys. Rev. **46**, 509 (1934).
[18] P. Ziesche, V. H. Smith, Jr., M. Ho, P.Gersdorf, M. Taut, J. Chem Phys. **110**, 6135 (1999).
[19] P. Fulde, Electron Correlations in Molecules and Solids, Springer, Berlin, 1995.
[20] W. Kutzelnigg, G. del Re, G. Bertier, Phys. Rev. **172**, 49 (1968).

---

*Corresponding author: okopin@fuw.edu.pl